https://doi.org/10.2352/issn.2169-2629.2020.28.44

Developing a multi-spectral imaging system using a RGB camera under two illuminations

Zhen Liu,[1,2,4] Kaida Xiao,[2,3] Michael Pointer,[2] and Changjun Li,[3]

[1] Shanghai Publishing and Printing College, China
[2] School of Design, University of Leeds, UK
[3]School of Computer Science and Software Engineering, University of Science and Technology Liaoning, China
[4]School of Statistics, Qufu Normal University, China
k.xiao@leeds.ac.uk

Abstract

This paper proposes a multi-spectral imaging system, developed using a commercial-grade camera, under two commonly used illumination. Rather than using conventional direct or diffuse light, the novelty of our method is to use a cross-polarized imaging system to eliminate glare and specular highlights. Two RGB images are captured under two different color temperature lighting conditions. An improved reflectance estimation method is developed to transform camera RGB under two illumination to spectral reflectance using a regulated model, combining the polynomial expansion of the camera signals with optimally selected feature. The method was tested using both a semi-gloss ColorChecker SG (140) and matte ColorChecker DC (240) chart. The results indicate that the proposed method significantly outperforms the traditional methods both in terms of spectra and colorimetric accuracy. This new multi-spectral imaging system is sufficiently precise to predict spectra properties and its performance within an acceptable range.

1 Introduction

One of the ultimate goals of spectra estimation from camera image is to predict spectral reflectance data that represent the physical properties from device dependent camera signal. Spectral reflectance is a major area of interest in many fields that include biometric identification[1], art archiving[2], the cosmetics industry[3], high fidelity color reproduction[4], etc. Thus, the technique of spectra estimation from camera images has gained in importance.

Generally, it is acknowledged that spectral reflectance estimation from a three channel RGB camera has a relatively less accuracy comparing with a multi-spectral imaging system that contains more signal channels. Conventionally, multi-spectral imaging system is constructed using a monochrome camera with narrowband filtration systems, for example, narrowband filter in front of camera [5-8], narrowband illumination imaging systems[9-12]. To reduce cost of multi-spectral camera, system with broadband filters with a trichromatic digital camera were developed [13-16]. Due to high cost and complicated system setup, multispectral camera system is still used in research laboratory in most case.

With dramatically developing technology for both digital camera and LED lightings, a multispectral imaging system with consumer-grade cameras with broadband lightings can be developed with much lower cost and easy operation processing, although the spectral reflectance estimation algorithm needs to be developed and verified.

The aim of this study is to develop a multispectral imaging system using a RGB camera and two commonly used illumination (D65 and white Fluorescent). We specially focused on the development of a more accurate spectral estimation method from raw camera responses using relatively simple approach. The regularization regression model [16-19]is used in this study. To solve overfitting problem, we develop a feature selection processing using neighborhood component analysis. The superior performance of this proposed method is evaluated and compared with existing methods by using both a semi-glossy ColorChecker SG (CCSG140) chart and a matte ColorChecker DC chart (CCDC240)，The overall performance of both the proposed and the traditional methods is compared in terms of both spectral and colorimetric accuracy.

2 Multispectral imaging system

2.1 Camera setup

The multispectral imaging system we developed includes a commercial trichromatic camera (Canon EOS 6D Mark II) with 16-bit digitization, two spectrally tunable THOUSLITE® LEDCubes. As shown in Figure 1, the imaging plane of digital camera was set to be approximately parallel to the sample placement plane and two THOUSLITE LEDCubes placed in approximately 45° to colour samples.

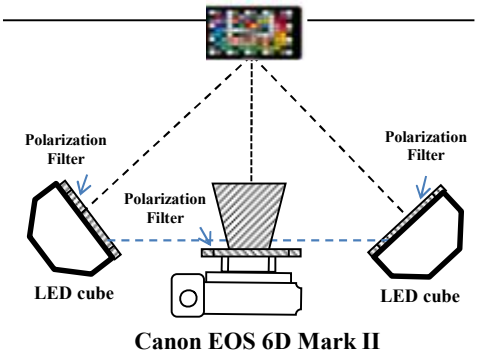

***Figure 1** the system setting of image acquirement*

During image capture, each cube is used to simulate D65 (CCT approximately 6500k) and a white fluorescent (CCT approximately 3500k), respectively. In order to eliminate glare and specular highlights from camera image, a linear polarizer was placed in front of each cube (Figure 2a) and a linear

polarizer filter was fitted in front of camera lens. The spatial non-uniformity of the light field was corrected using exposure to a white card. Relative spectral power distribution of two illumination was measured using a diffused white sample and illustrated in Figure 2b.

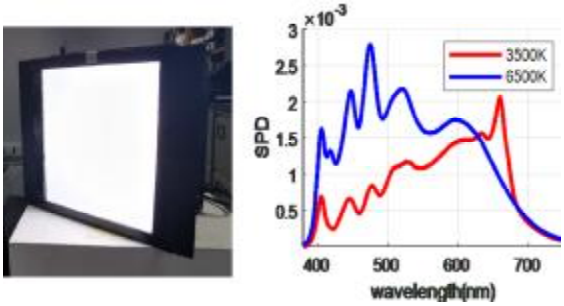

Figure 2 *LEDCube and SPD curves of 3500K and 6500K illumination*

The parameters setting for the camera were fixed during the image capture, with the aperture size as f5.6, the shutter speed of 1/8 second, and the ISO as 640. The Canon EOS utility software was used to control the camera for image capture. Camera raw RGB data was recorded and used to predict spectral reflectance. The dark current noise was recorded with camera lens cap closed and was subsequently subtracted from captured digital images.

2.2 Spectral reflectance estimation

2.2.1 Regularization model

Regularizaion model has been widely used for reflectance estimation from camera image [16-19] and it is also used in this study.

The camera response is proportional to the intensity of the captured light; thus the camera response can be expressed as a linear combination of the camera sensitivity functions, the illumination spectral power distribution, and spectral reflectance of objects. As has been shown [4-10], the camera sensor response vector c can be related to spectral reflectance:

$$c = LSr + \varepsilon \tag{1}$$

where, L is a diagonal matrix representing the spectral power distribution of illuminant, S is a matrix representing the spectral sensitivities of sensors, r is a discrete spectral vector of the object uniformly sampled over the visible wavelength range from, typically 400 nm to 700 nm at 10 nm intervals, $\mathcal{E}$ is the additive system error not only from the camera sensor itself but also measurement errors associated with the spectral characteristics of the sensors, illuminant and objects.

The spectral reflectance can be estimated using prior knowledge by a training-set of measured color patches and the camera responses. When the error can be ignored, the above equation can be transformed as a scalar product in matrix notation as:

$$R = C\Theta \tag{2}$$

where R is a matrix of the spectral dataset in which each row represents the spectral reflectance of a sample, C is *the* camera response matrix and each row of it consists of one or two sets (two tree channel images taken under two different lighting conditions) of camera response for a sample, Θ is a transform matrix between the camera response and the spectral reflectance.

As described in the literature, most spectral estimation processes perform the spectral estimation based on nonlinear regression models, including linear, second-, third-, and fourth-order polynomial expansion models. In general, the accuracy of spectra estimation depends not only on the training set but also on the number of signal features: the greater the number of features, the better the linearity of the imaging system. In order to improve the spectral estimation accuracy, a polynomial transform was used to extend the response values instead of increasing the number of imaging channels. Taking a 3rd order polynomial model as an example, six channel camera response (a row of C) can be extended to 84 terms:

$$\bar{C} = \begin{bmatrix} 1, R_1, G_1, B_1, R_2, G_2, B_2, R_1^2, R_1G_1, \cdots \\ G_2B_2, B_2^2, \cdots, R_1^3, R_1^2G_1, R_1^2B_1 \cdots B_2^3 \end{bmatrix} \tag{3}$$

Using $\bar{C}$ to denote the expended matrix from C , models can be built to map the polynomial camera response features to spectral reflectance as

$$R \approx \bar{C}\Theta \tag{4}$$

where, Θ is transform matrix to be searched for in the least-squares sense. This could address some of the problems by imposing a penalty on the size of the coefficients. The L_2-norm of the vector κ can be added to the loss expression in order to give preferred solutions with smaller norms. The objective functions of the form as follows:

$$J(\Theta) = \arg\min\left(\left\| \bar{C}\Theta - R \right\|_2^2 + \kappa \left\| \Theta \right\|_2^2 \right) \tag{5}$$

Here, κ is a regularization parameter to be empirically selected. The purpose of this regularization setting is to stabilize the regression output, which prevents a large change in the result at small perturbations in the input camera response. The gradient for the objective functions in the least-square sense becomes:

$$\begin{aligned} \frac{\partial J(\Theta)}{\partial \Theta} &= \frac{\partial}{\partial \Theta}((\bar{C}\Theta - R)^H(\bar{C}\Theta - R) + \kappa\Theta^H\Theta) \\ &= \bar{C}^H\bar{C}\Theta - \bar{C}^H R + \kappa\Theta \end{aligned} \tag{6}$$

Let the gradient manually be zero, that is $\frac{\partial J(\Theta)}{\partial \Theta} = 0$,

$$\Theta = (\bar{C}^H\bar{C} + \kappa I)^{-1}\bar{C}^H R \tag{7}$$

where κ is the parameter and I is the identity matrix. Small, positive values of κ reduce the variance of the estimates. While biased, the reduced variance of ridge estimates often results in a smaller mean squared error when compared to ordinary least-squares estimates. Referring to the singular value decomposition of expanded camera signal response matrix , $\bar{C} = U\Sigma V^H$, and $\bar{C}^H\bar{C} = V\Sigma^H\Sigma V^H$, $\delta_{\min}$ is the smallest positive singular value. the above equation can be transformed:

$$\Theta = V(\Sigma^H\Sigma + \delta_{\min}^2 I)^{-1}\Sigma^H U^H R \tag{8}$$

2.2 Feature Select for Polynomial Expansion

It should be noted that, when the number of polynomial expansion signals is large, its components are correlated, and the columns of the signal matrix have an approximate linear dependence. The estimation is extremely sensitive to random noise in the camera response, producing a large variance, and

the situation of multi-collinearity would be an issue. This will degrade the prediction performance and the stability of spectra estimation precision [20]. The objective of a feature selection search for a subset of extended polynomial camera responses, optimally models between the camera responses and the spectral reflectance. The subset is subject to constraints such as required or excluded features, and the size of the subset. The performance of the spectral estimation transform matrix can be improved using neightborhood component analysis feature selection [21-22]. Here, the Matlab function *fsrnca*, in the Machine Learning Toolbox, was used. Consider a spectral estimation training set S containing n color patches:

$$S = \{(c_i, r_i), i = 1, 2, 3 \cdots n\} \tag{9}$$

where c_i is polynomial expansion of the camera signals from the i^{th} patch, r_i is the corresponding spectral reflectance. A randomized regression model can be build that:

a. Randomly picks a patch *Ref(c)* from S as the 'reference point' for camera response c.
b. Sets the response value at c equal to the response value of the reference point *Ref(C)*.

The probability $P(Ref(x)=c_j|S)$ that point c_j is picked from S as the reference for c is

$$P\left(Ref(c) = c_j \mid S\right) = \frac{k(d_w(c, c_j))}{\sum_{j=1}^{n} k(d_w(c, c_j))} \tag{10}$$

where d_w is distance function, k is kernel function that assumes large values when d_w is small, Now consider the leave-one-out application of this randomized regression model, that is, predicting the response for c_i using the data in S^{-i}, and the training set S excluding the point (c_i, r_i). The probability that point c_j is picked as the reference point for c_i is given by:

$$p_{ij} = P(ref(c_i) = c_j \mid S^{-i}) = \frac{k(d_w(c_i, c_j))}{\sum_{j=1, j\neq i}^{n} k(d_w(c_i, c_j))} \tag{11}$$

Let $\tilde{r}_i$ be the response value the randomized regression model predicts and r_i be the actual spectral response for c_i. And let l be a loss function that measures the disagreement between r_i and $\tilde{r}_i$. Then, the average value of the loss function $l(r_i, \tilde{r}_i)$ is given by:

$$l_i = E(l(r_i, \tilde{r}_i) \mid S^{-i}) = \sum_{j=1, j\neq i}^{n} p_{ij} l(r_i, \tilde{r}_i) \tag{12}$$

After adding the regularization term λ, the weight vector w can be expressed as the following minimization regression error,

$$\hat{w} = \arg\min_{w} \{f(w)\} = \arg\min_{w} \{\frac{1}{n}\sum_{i=1}^{n} l_i + \lambda \sum_{r=1}^{p} w_r^2\} \tag{13}$$

Where, w_r is weight vector for r^{th} feature item, n is the number of observations, and p is the number of predictor variables.

3 Results and Discussions

3.1 Experiment

To verify the proposed approach, comparative experiments were conducted. An X-Rite® ColorChecker semi-gloss chart (CCSG, 140 patches) and a Gretag-Macbeth ColorChecker DC matte chart (CCDC, 240 patches including 232 matte, and 8 glossy patches) were used as color targets and captured by the proposed multi-spectral imaging system. Raw camera RGB of each patch in the colour chart was obtained. All the patches were divided into five groups and for each group, 4/5th of the patches were assigned as a training set, and 1/5th of the patches as a test set. The spectral reflectance of all the patches was measured by use of a Konica-Minolta CM-2600d spectrophotometer with an interval of 10 nm over the wavelength from 400 nm to 700 nm (under SCE measurement based on d/8 geometry). Both spectra difference and colour difference between model predicted results from camera and the measurement results from the spectrophotometer were calculated to represent performance of predictive accuracy for spectral reflectance estimation.

3.2 Feature selection

Neighborhood component analysis feature selection is performed to optimize feature selection for proposed imaging system. By selecting weighted features, the colorimetric and spectral metric precision will be determined as the feature number is changed. In this study, using 380 color samples from the SG140 chart and DC240 chart, a regularization model with 3rd order polynomial expansion was used to calculate the different selected features in terms of both the spectral reflectance RMSE and the mean CIELAB color difference. Figure 3 was plotted to illustrate the relationship between the mean spectral reflectance RMSE, the mean CIELAB color difference and the features numbers within the expanded polynomial feature range. It is found that the performance of colorimetric metric and spectral metric initially decreased with an increase in feature number, and then they increase after they reach an optimal value of about 30. Furthermore, it is clear from Figure 3 that the evaluation metrics of both RMSE and CIELAB color difference show the same trend with the changes in feature number, therefore, the proposed method can simultaneously minimize the spectral and colorimetric errors. Too many items, however, may cause the over-fitting problems as explained by Urban et al. [13]. Thus, it should be more meaningful to understand the importance of the features and train a model using the only selected features.

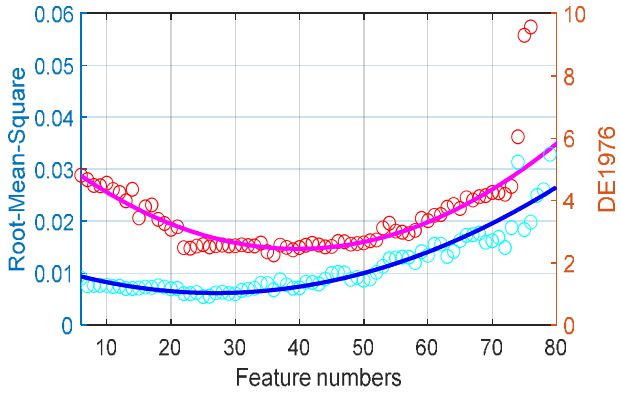

Figure 3 *The relationship between number of features and spectral and color performance*

Figure 4(a) illustrates the feature selection weights of 84 extended 3rd order polynomial feature items from six-channel camera responses using neighborhood component analysis (NCA). Over half the feature weights are nonzero. Calculating the loss using the test set as a measure of the performance, the

weights of the irrelevant features should be close to zero and improve the performance for feature selection using five-fold cross-validation. Figure 4(b) shows a hierarchical treemap view of feature weights and shows the obvious patterns: including which items are most important for spectral estimation. The relationship between each feature is shown by color and proximity. The 30 most relevant features were identified and are summarized in Table 1. There are 6 1st order terms, 17 2nd order terms, and 7 3rd order terms that are most important for spectral estimation. This means that not all terms are necessary for spectral estimation; part of the 2nd order and 3rd polynomial expansion are negative and irrelevant and decrease the estimation performance.

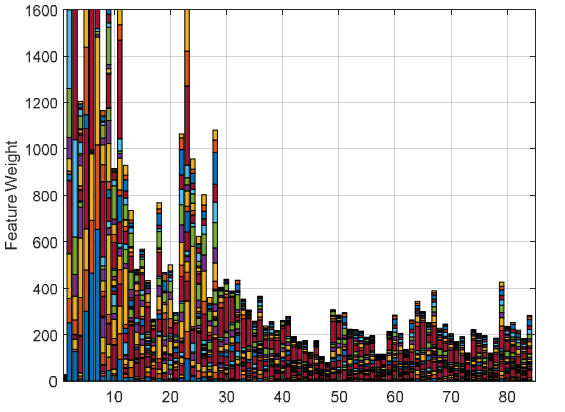

(a) Feature weight

(b) hierarchical treemap view

***Figure 4** Feature selection among 84 items for 3rd polynomial expansions*

Table 1 Selected terms of the polynomial regression

Order	Polynomial regression
1st order (6)	$R_1, G_1, B_1, R_2, G_2, B_2$
2nd order (17)	$R_1^2, G_1^2, B_1^2, G_2^2, R_2^2, R_1B_1, R_1G_1, R_1R_2, R_1G_2, B_1G_2$ $B_1R_2, B_1G_1, G_1R_2, G_1G_2, R_2B_2, R_2G_2, B_2G_1$
3rd order (7)	$G_1G_2^2, G_1^2G_2, B_1G_1^2, G_1^3, G_2^2R_1, G_2R_1^2, R_1^3$

3.3 Model performance

Based on proposed multi-spectral camera system, the performance of spectral reflectance estimation for regulated model with different expansions (including 1st order polynomial expansion, 2nd order polynomial expansion, 3rd order polynomial expansion and 4th order polynomial expansion and finally 3rd order polynomial expansion with proposed 30 feature selection) were evaluated in terms of both colorimetric error and spectral diffierence respectively. All results are given in Table 2: the average performance, the maximum and minimum error are shown in Root-means-square errror (RMSE), goodness fitting coefficient (GFC)[15], and CIE CIELAB 1976 color difference under 5 testing illuminations (including 3500K, TL84, D50, D55 and D65).

Table 2 Performance of reflectance estimation using two illuminants with different polynomial expansion

	RMSE(%)			GFC(%)			CIELAB DE		
	avg	max	min	avg	max	min	Avg	max	min
1st 7	3.0	11.0	0.8	99.5	99.9	95.0	2.6	7.9	0.6
2nd 28	3.1	10.4	0.4	99.8	99.9	98.3	2.3	6.5	0.3
3rd 84	2.9	9.9	0.4	99.8	99.9	98.5	2.4	8.5	0.4
4th 210	3.1	9.3	0.2	99.8	99.9	98.3	2.3	7.5	0.3
Selected 30	2.2	7.3	0.3	99.8	99.9	98.6	2.2	5.5	0.3

It can be seen from Table 2, the best performance, i.e. the smallest average color difference between the predicted and the measured spectral, is achieved by selected 30 features items from 3th order polynomial expansion. The average CIELAB color difference is approximately 2.2 ΔE^*_{ab} and root-mean-square error is 2.2. This all indicate that our feature selected method is outperforms the traditional expansion methods both in terms of spectral and colorimetric accuracy.

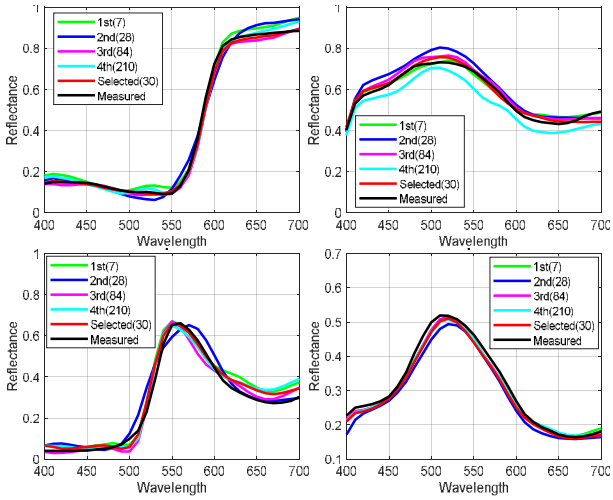

***Figure 5** Representative samples of reconstructed spectra with different polynomial expansions*

In order to investigate whether RGB camera under two illumination can give a better spectra estimation than that under one illumination, Regularization model with third order polynomial regression is also conducted for camera signal under each illumination (3500k or 6500k). Performance of spectra estimation for RGB camera under 3500k, RGB camera under 6500k, RGB camera under both 3500k and 6500k without feature selection (84 items), RGB camera under both 3500k and 6500k with feature selection (30 items) were listed in Table 3 in terms of the average, maximum and minimum error and standard deviation by the CIELAB color differences under five tested illumination. Root-mean-square errors between estimated and measured spectral reflectance were also calculated and the mean results for each model is also listed in Table 3. It can be seen that the best performance, i.e. the smallest average color difference and RMSE between the predicted and the measured spectral, is achieved by our

proposed method, which uses 30 items from the 3rd order polynomial expansion variables and 6 channels under both 3500 K and 6500 K illumination. Thus, the method achieves improved estimation accuracy by selecting features from polynomial expansion of camera response under two illumination conditions.

Table 3 Performance of the four reconstruction methods across different illuminants (CIE 1931，380 patches, 80% train, 20% test, extended 3rd order polynomial)

		3500 K (20)	6500 K (20)	3500 K & 6500 K (84)	3500 K & 6500 K (30)
ΔE^*_{ab}	Mean	2.73	2.56	2.4	2.27
	max	7.65	6.22	8.79	5.4
	min	0.26	0.22	0.36	0.09
	Std	1.74	1.47	1.75	1.21
RMSE	Mean	2.78%	2.80%	2.65%	2.56%
	max	7.83%	7.28%	9.86%	8.34%
	min	0.45%	0.32%	0.38%	0.31%
	Std	1.80%	1.78%	2.30%	1.60%

3.4 Discussion

In his study, we developed a multispectral camera system using two commonly used illumination and proposed new method to improve the accuracy of estimation of spectral data from the raw camera responses. The results illustrate that performance of reflectance estimation from camera image can be significantly improved when two broadband illumination is used. This implies multi-illumination with coconsumer-grade camera can be an effective approach to construct a multi-spectral camera system.

We found the feature selection of the expanded camera response influences the estimation performance. Even more interestingly, a small number of feature can provide a better performance than full selection of feature for camera response expansion. The selection of feature might depends by camera, illumination and possibly training dataset. Further investigation of factors affecting feature selection will be conducted and reported in the full paper.

4. Conclusions

This paper proposes a new multi-spectral imaging system using a RGB camera under two illumination. Method for spectra estimation from raw camera responses by feature selected expansion items under two illumination conditions is developed. The performance of the proposed method is evaluated using ColorChecker charts. The results show that proposed method can give good accuracy in terms of both the spectral and colorimetric estimation.

References

[1]. Uzair, M, Is spectral reflectance of the face a reliable biometric?, Optics Express, 12,23, pg. 15160-15173(2015).

[2]. Berns, R, High-Accuracy Digital Imaging of Cultural Heritage without Visual Editing. Porc Archiving 2005(2005).

[3]. Kikuchi, K., et al Imaging of hemoglobin oxygen saturation ratio in the face by spectral camera and its application to evaluate dark circles, Skin Research and Technology, 4,19 pg. 499-507 (2013).

[4]. Hardeberg, J.Y., Acquisition and Reproduction of Color Images: Colorimetric and Multispectral Approaches. Ecole Nationale Superieure des Telecommunications: Paris, France pg. 324 (1999).

[5]. Helling, S., et al. Algorithms for spectral color stimulus reconstruction with a seven-channel multispectral camera. Proc Colour in Graphics, Imaging, and Vision. (2004).

[6]. Mathews, S.A., Design and fabrication of a low-cost, multispectral imaging system, Applied optics, 47, pg. 71-76 (2008).

[7]. Hardeberg, J.Y, et al Multispectral color image capture using a liquid crystal tunable filter, Optical Engineering, 41,pg. 2532-2548(2002).

[8]. Shen, H.L., et al., Reflectance reconstruction for multispectral imaging by adaptive Wiener estimation. Optics Express, 15, 23, pg. 15545-15554(2007)

[9]. Han, S., et al., Fast spectral reflectance recovery using DLP projector. International journal of computer vision, 110,2, pg. 172-184(2014).

[10]. Jiang, J. and J. Gu. Recovering spectral reflectance under commonly available lighting conditions. Proc IEEE.Computer Vision and Pattern Recognition Workshops. (2012).

[11]. Tominaga, S. and T. Horiuchi, Spectral imaging by synchronizing capture and illumination, JOSA A, 29, 9, pg. 1764-1775(2012).

[12]. Zhang, X., et al., Estimating spectral reflectance from camera responses based on CIE XYZ tristimulus values under multi-illuminants, Color Research & Application, 42,1, pg. 68-77(2017).

[13]. Urban, P., M.R. Rosen, and R.S. Berns, Spectral image reconstruction using an edge preserving spatio-spectral Wiener estimation. JOSA A, 26, 8, pg. 1865-1875(2009)

[14]. Zhao, Y. and R.S. Berns, Image-based spectral reflectance reconstruction using the matrix R method. Color Research and Application, 32,5,: pg. 343-351(2007).

[15]. Liu, Z., et al., Optimized spectra estimation based on adaptive training set selection. Optics Express, 25,11, pg. 12435-12445(2017).

[16]. Ke, W., et al., Medical imaging based spectral reflectance reconstruction combining PCA and regularized polynomial. Biomedical Research, pg381-383(2018).

[17] W. Menke, Geophysical Data Analysis: Discrete Inverse Theory (Academic, 1989).

[18] Xiao K, Zhu Y, Li C, Connah D, Yates JM, Wuerger S. Improved method for skin reflectance reconstruction from camera images. Optics Express. 24(13), pg. 14934-14950 (2016)

[19] Liang J, Xiao K, Pointer MR, Wan X, Li C. Spectra estimation from raw camera responses based on adaptive local-weighted linear regression. Optics Express. 27(4), pg. 5165-5180(2019)

[20] Guyon, I. and A. Elisseeff, An introduction to variable and feature selection. Journal of Machine Learning Research 3(8): pg. 1157-1182(2003).

[21] Von Luxburg, U., A tutorial on spectral clustering. Statistics and Computing 17(4): pg. 395-416(2007).

[22] Yang, W., K. Wang, and W. Zuo, Neighborhood Component Feature Selection for High-Dimensional Data. Journal of Computers, 7(1): pg. 161-168(2012).

Author Biography

Zhen LIU received his Ph.D. in Graphic communication engineering from Wuhan University, China, in 2012. Currently she is working in the Institute of Color vision and Imaging, Qufu Normal University. His work focuses on multispectral imaging, Color restoration of faded relics.